http://dx.doi.org/10.1002/chem.200401133

J. Schmedt auf der Günne, J. Beck, W. Hoffbauer, and P. Krieger-Beck. The structure of poly(carbonsuboxide) on the atomic scale - a solid-state NMR study. *Chem. - Eur. J.*, 11:4429--4440, 2005.

The Structure of Poly(carbonsuboxide) on the Atomic Scale - A Solid-State NMR Study

Jörn Schmedt auf der Günne,* Johannes Beck, Wilfried Hoffbauer, Petra Krieger-Beck

Institut für Anorganische Chemie der Universität Bonn,

Gerhard Domagk-Straße 1, 53121 Bonn, Germany

7th March 2005

*corresponding author; Email Address: gunnej@uni-bonn.de

Abstract

In this contribution we present a study of the structure of amorphous poly(carbonsuboxide) $(C_3O_2)_x$ by ^{13}C solid-state NMR supported by infrared spectroscopy and chemical analysis. Poly(carbonsuboxide) was obtained via polymerization of carbonsuboxide C_3O_2, which in turn was synthesized from malonic acid bis(trimethylsilylester). Two different ^{13}C labeling schemes were applied to probe inter- and intramonomeric $C-C$ bonds in the polymer by dipolar solid-state NMR methods and also to allow quantitative ^{13}C MAS NMR spectra. Four types of carbon environments can be distinguished in the NMR spectra. Double-quantum and triple-quantum 2D correlation experiments were used to assign the observed peaks using the through-space and through-bond dipolar coupling. In order to obtain distance constraints for the intermonomeric $C-C$ bonds, double-quantum constant-time experiments were performed. In these experiments an additional filter step was applied to suppress contributions from not directly bonded $^{13}C-^{13}C$ spin pairs.

The ^{13}C NMR intensities, chemical shifts, connectivities and distances gave constraints for both the polymerization mechanism and the short-range order of the polymer. The experimental results were complemented by bond distances predicted by density functional theory methods for several previously suggested models. Based on the presented evidence we can unambiguously exclude models based on γ-pyronic units and support models based α-pyronic units. The possibility of planar ladder like and bracelet like α-pyronic structures is discussed.

keywords: structure, poly(carbonsuboxide), solid-state NMR, C_3O_2 , polymer, DFT, MAS, amorphous

1 Introduction

At room temperature carbonsuboxide C_3O_2 is a metastable gas which readily polymerizes to a brown/red amorphous solid $(C_3O_2)_x$ as discovered by Diels in 1906 [1]. Since then both the polymer and the monomer have received much attention. While chemists were interested in the polymerization process, its structure, physical properties and reactivity, astrophysical scientists perceive it as a source of extraterrestrial carbon in comets [2] and perhaps on the surface of Mars or Venus [3].

The monomer C_3O_2 has a low melting point of -112.5 °C and a boiling point of +6.8 °C [4]. Its crystal structure [5] was solved only recently showing slight deviations from linearity O=C=C=C=O. The singular electronic structure of carbonsuboxide is the reason for its high reactivity in many different reactions but also for the difficulties in its synthesis especially when high yields are required. The highest yields have been achieved via thermolysis of the malonic acid bistrimethylsilylester on P_4O_{10} at 160 °C [6].

The polymer $(C_3O_2)_x$ can be obtained via chemical vapor deposition from the gas-phase [7–10], via gamma-ray initiation from the solid [11, 12] or using different means of initiating the polymerization reaction from liquid phase [12–14]. The polymerization occurs even without adding a starting agent. Traces of acid or even absorbed water on the surface of a glass vessel are initiating the transformation reaction in these cases [15]. Polymerization at ambient temperature yields a product $(C_3O_2)_x$ of well defined stoichiometry. At elevated temperatures it is well known that the polymer loses carbonmonoxide and carbondioxide [9, 10] leaving a graphite-like carbonoxide with low oxygen content at temperatures of about 700 °C.

The polymerization is an exothermic reaction (-136 kJ/mole) [16]. The gas phase and bulk reaction were found to follow a rate equation being first order both with respect to polymer and monomer concentrations [17, 18]. Activation energies vary with different surface materials from 1.5 to 2.4 kJ/mole [7, 13, 17].

A very difficult issue is the elucidation of the molecular structure of poly(carbonsuboxide)s. Their amorphous character and insolubility in many organic solvents are the main reasons why so many contradictory structural models can be found in the literature [10, 12, 14, 18, 19]. Even worse, there are indications that poly(carbonsuboxide) polymers with different molecular structure

do exist. An early model suggested by Diels described the polymer as a spiropolycyclobutadione [15], Ziegler [20] described the structure as a poly-α-pyrone, Boehm et al. [14] suggested a single planar molecule formed by about 15 monomers units and Paiaro et al. [12] polymers based on poly-γ-pyrone or a mixed α-pyrone and γ-pyrone backbone, respectively. In patent literature even claims of cyclopoly(carbonsuboxide)s are made [19].

Various analytical methods have been used so far to obtain structural information about the amorphous polymer, e.g. IR, UV/VIS [7–10,13,14], X-ray diffraction [8], molar mass determination [12], pyrolysis [9, 10, 12], titration of acidic groups, EPR spectroscopy [7, 11, 13] and chemical analysis to determine the composition of the polymer. IR allowed to identify some basic building units, for example carbonyl-functions, ethenyl and ketene units, without being able to quantify their portion. X-ray diffraction gave some vague indications of the ring sizes. UV/VIS spectra indicated extended π-systems to be present in the polymer. EPR spectra proved the existence of unpaired electrons in the polymer, which seems to be linked to the availability of ketene units. Carbon monoxide and dioxide which evolve during pyrolysis gave indirect evidence of the molecular structure. It should be noted that both titration of the acid centers and determination of the molar mass required a solution of the analyte, which is a delicate issue in case of the almost insoluble poly(carbonsuboxide). Despite a consensus in the older literature that the polymer backbone is made of poly-α-pyrone convincing quantitative evidence is not available. Consequently more recent experimental evidence [12] questions the simple poly-α-pyrone model. In addition it has been shown by small angle X-ray scattering on solutions of poly(carbonsuboxide) [21] that the molar mass has been greatly underestimated in earlier work [8, 12, 13].

Being an element-selective, inherently quantitative method with excellent local resolution power, solid-state NMR has shown great promise as a structural tool of characterizing disordered solid state materials [22]. In the case of poly(carbonsuboxide) solid-state NMR requires ^{17}O or ^{13}C enriched materials, which then also allows the use of modern dipolar NMR methodology. Connectivity and spatial proximity can be studied via multi-dimensional multiple-quantum NMR methods [23]. ^{13}C-^{13}C internuclear distances can be determined via double-quantum experiments [24–27].

In this contribution we are presenting results from ^{13}C solid-state NMR spectroscopy probing the molecular structure of poly(carbonsuboxide) polymerized at room temperature via spontaneous

polymerization. NMR is used to identify and quantify functional groups present in the polymer making use of the well established structural correlation of the ^{13}C chemical shift scale and multidimensional double-quantum and triple-quantum NMR. Polymers with two different ^{13}C labeling schemes were prepared which allow to study the entanglement of the monomers and allow to probe if the integrity of the monomers during reaction is preserved. A double-quantum double-filtering scheme is introduced which allows to measure distances in heavily labeled materials, needed here to obtain internuclear distances. Infrared spectroscopy and chemical analysis complement the NMR results which allows us to discuss the structural perception of poly(carbonsuboxide) on a molecular level. The article is organized such that in the experimental part technical details for the synthesis, IR-, NMR-experiments, NMR-methodology and computational details are given, while the following parts focus on the discussion of the results in terms of different models of the local structure.

2 Experimental Section

2.1 Sample Preparation and Characterization

Carbonsuboxide C_3O_2 was prepared by thermolysis of the bis(trimethylsilylester) of malonic acid in presence of P_2O_5 at 160 °C [6]. C_3O_2 was caught in a cryo trap at liquid N_2 temperature and distilled twice at dry ice temperature.

For polymerization 1 to 2 ml of C_3O_2 were condensed into glass ampules (150 mm length, 15 mm inner diameter and 2 mm wall thickness) onto 3 ml dry CCl_4. The ampules were cooled down to liquid nitrogen temperatures and sealed by melting. The transformation to the polymer is complete within five days of keeping the ampule at room temperature. The polymer is a red-brown voluminous fine powder.

For opening of the reaction vessels the content was frozen with liquid N_2 and the ampules were broken under an atomsphere of argon. The solvent CCl_4 was distilled off in a vacuum at ambient temperature. After 24 hours of continuous pumping the vapour pressure reached 10^{-3} mbar. Then the opened ampules were transferred to the argon-filled glove box.

Isotopically labeled carbonsuboxide was prepared, starting from isotopically labeled malonic acid. The educts $[1,2,3-{}^{13}C_3]$, $[2-{}^{13}C]$ and $[1,3-{}^{13}C_2]$ malonic acid (each position labeled to

~99%) were obtained from Cambridge Isotope Laboratories and converted to the bis(trimethylsilylesters). Two polymers with the following labeling schemes were realized. Given are the mixtures of carbonsuboxides before polymerization (percentages reflect the mass ratio):

Educts for **sample I**: 15% $\left[1,2,3-{}^{13}\mathrm{C}_3\right]-\mathrm{C_3O_2}$ and 85% $\mathrm{C_3O_2}$ (with natural abundance)

Educts for **sample II**: 16.67% $\left[1,3-{}^{13}\mathrm{C}_2\right]-\mathrm{C_3O_2}$, 33.33% $\left[2-{}^{13}\mathrm{C}\right]-\mathrm{C_3O_2}$ and 50% $\mathrm{C_3O_2}$(with natural abundance)

Note: Carbonsuboxide is lacrymonious and needs to be handled with care. Both poly(carbonsuboxide) and carbonsuboxide are strongly hygroscopic, hence all operations were performed in a glove box under argon atmosphere.

The average chemical composition of the polymers was determined via combustion analysis to $\frac{m(\mathrm{C})}{m_{total}} = 0.503$, $\frac{m(\mathrm{H})}{m_{total}} < 0.003$, $\frac{m(\mathrm{N})}{m_{total}} < 0.004$ which corresponds to an approximate sum formula of $(\mathrm{C_3O_2})_x$, with a small amount of absorbed water. The purity of the monomeric $\mathrm{C_3O_2}$ was also checked [28] by ^{13}C liquid-state NMR on a BRUKER DPX 300 (^{13}C NMR (in $\mathrm{CDCl_3}$) δ 130.5, -15.1 ppm, $\left|{}^1J(\mathrm{C}-\mathrm{C})\right| = 174.9\,\mathrm{Hz}$). The ^{13}C enrichment on different carbon positions of the malonic acid was checked via mass spectrometry.

Chemical analysis of the polymers was in agreement with the composition $\mathrm{C_3O_2}$. The polymer $(\mathrm{C_3O_2})_x$ in our experience is only partially soluble in all absolutely dry solvents which impedes molar mass determination by standard techniques. Already small amounts of water increase solubility drastically. A determination of the molar mass and molecular shape of the dissolved polymer in DMF/$\mathrm{H_2O}$ by small-angle X-ray scattering has recently been performed [21].

2.2 Infrared Spectroscopy

Infrared spectra were obtained with a BRUKER IFS 113 spectrometer at room temperature. The samples were pressed with anhydrous KBr to pellets.

2.3 Solid-State NMR

2.3.1 General

The ^{13}C NMR experiments were carried out on a Varian Infinity+ NMR spectrometer equipped with a commercial 4 mm double-resonance MAS-NMR probe. The magnetic field strength was 9.4 T corresponding to a resonance frequency $\nu\left(^{13}\mathrm{C}\right) = 100.29\,\mathrm{MHz}$. Samples were rotated within zirconia spinners. By means of appropriate spacers, the sample was confined to the middle $1/3$ of the rotor volume. A commercially available pneumatic control unit was used to limit MAS frequency variations to a ± 2 Hz interval for the duration of the experiment.

For multiple quantum experiments the probe was tuned by minimizing the reflection of high-power pulses. C-sequences applied a pulse nutation frequency of 70 kHz, readout pulses a nutation frequency of 100 kHz. Spin-lattice time constants were measured using the saturation-recovery technique. All multiple-quantum experiments were preceded by a pulse comb of $10-20$ 90°-pulses and intermittent dephasing delays of 20 ms to prevent intersequence echoes.

2.3.2 ^{13}C MAS NMR 2D-Correlation Spectroscopy

Double-quantum and triple-quantum 2D-correlation spectra were acquired with rotor-synchronized INADEQUATE pulse-sequences [29] sketched out in figure 2 (pulse-sequences A and B). This scheme allows selective through-bond excitation of double-quantum coherences and hence is very useful detecting directly bonded nuclei. The corresponding double- and triple-quantum filtered 2D correlation spectra in figures 6 and 7 were acquired at a spinning-speed of $\nu_r = 15\,\mathrm{kHz}$ and $\nu_r = 10\,\mathrm{kHz}$ and a conversion time of $\tau^J_{DQ} = 6.0\,\mathrm{ms}$ and $\tau^J_{TQ} = 7.0\,\mathrm{ms}$, respectively. In addition we have performed 2D-correlation spectroscopy based on the through-space dipolar coupling. Acquisition of the indirect dimension (labeled t_1) was rotor synchronized in all cases, typically sampling the indirect dimension with 16 time increments. For frequency sensitive detection we used the States approach [30], i.e. acquiring a second set with a constant phase offset on double-quantum or triple-quantum reconversion pulses of 45° and 30° respectively. 2D double-quantum correlation spectroscopy based on supercycled R-sequences [26] was performed to establish the spatial neighborhood of carbon atoms under fast spinning conditions. In comparison to the double-quantum

pulse-sequence in figure 2 the INADEQUATE blocks have to be replaced by compensated blocks of $\left[\mathrm{R}14_4^5, \mathrm{R}14_4^{-5}\right]$ units where R describes a composite pulse $\mathrm{R} = \{90_{180}, 270_0\}$. The notation 90_{180} describes a pulse with 90° flip angle and 180° pulse phase. For a detailed description of this method consult the literature [24, 26]. The 2D spectra in figures 5 and 8 were obtained using 56 R-elements and a spinning-speed of 15 kHz.

Coherence pathway selection was done phase-cycling the pulse-phases only, thus keeping the receiver phase constant. Phases were determined according to cogwheel phase-cycling [31] with 12 steps for double-quantum filtered spectroscopy and with a difference in winding numbers between the excitation and reconversion block $\Delta\nu_{12} = 3$ and between the reconversion block and read pulse $\Delta\nu_{23} = 1$, which amounts to a $\mathrm{Cog}12(2,5,6;0)$. Thus the pulse phase increments ϕ in the i-th experiment for double-quantum excitation, reconversion and the read pulse block have been written out in reference [24].

The phase cycle selects the coherence transfer pathways $0 \rightarrow +2 \rightarrow 0 \rightarrow -1$ and $0 \rightarrow -2 \rightarrow 0 \rightarrow -1$ as indicated in figure 2, neglecting all coherence pathways which involve coherence orders $|p| > 2$. An additional 4 step phase cycle realizes DC offset and quadrature image compensation. The triple-quantum filtered spectroscopy experiments were done accordingly using a $\mathrm{Cog}24(7,11,12;0)$.

Typical repetition rates for the 2D-experiments varied between 64 s and 640 s.

2.3.3 Constant-Time Double-Quantum NMR

In double-quantum filtered spectroscopy the nuclear spin-system evolves under a purely dipolar average Hamiltonian for a conversion time τ_{DQ}. The double-quantum filtered efficiencies which are measured from a set of experiments with variable excitation and reconversion times, τ_{DQ}^{exc} and τ_{DQ}^{reconv} respectively, then show oscillations depending on the through space dipole-dipole coupling interaction only. In the limiting case of simple 2-spin systems internuclear distances can be determined with good accuracy. In this context the constant-time data sampling approach helps to reduce the number of unknown variables to fit the experimental curves [24]. This is achieved by keeping the sum of excitation and reconversion time constant $\tau_{DQ}^{total} = \tau_{DQ}^{exc} + \tau_{DQ}^{reconv}$.

Here we make use of constant-time double-quantum NMR to determine distances in a heavily labeled material. More specifically we are interested in the distance between the carbon atoms link-

ing two different monomer units in the resulting polymer (see figure 11). In good approximation one may still describe the ^{13}C spin system of **sample II** as consisting of ^{13}C $-^{13}$C spin-pairs. However in contrast to selectively labeled crystalline materials, there are also ^{13}C $-^{13}$C spin-pairs which are not directly bonded (see figure 3) and thus have a bigger internuclear distance. With the simple double-quantum pulse-sequence displayed in figure 2-C it is difficult to differentiate between contributions of those spin-pairs which are directly bonded and those which are not (compare figure 3). One may however utilize the fact that only the directly bonded spin-pairs have a sizeable J coupling constant. A very simple scheme for the suppression of indirectly bonded spin-pairs is an additional double-quantum filter step based on the J coupling mediated INADEQUATE experiment. The resulting pulse-sequence is described in figure 2-D and consists of four double-quantum conversion steps, two of them based on the J coupling interaction, two based on the through-space interaction. This experiment will be termed double-quantum constant-time double-filtering in the following and is familiar to an experiment recently reported by Saalwächter et al. [32].

The double-quantum filter was optimized independently on pulse-sequence A (see figure 2) for maximum efficiency to $\tau_J = 6.8\,\text{ms}$ using a repetition delay of 64 s. Coherence transfer pathways were selected with a nested 256 step phase cycle changing the phases of each double-quantum conversion block in cycles of 4 steps independently. In principle a 16-step phase cycle would be sufficient if z-filtering and active rotor synchronization can be applied. The two conversion blocks acting as a through-space dipolar-coupling filter were implemented according to PostC7 [33] ($C7_2^1$,with a $\left[C7_2^1\right]_{+0}\left[C7_2^1\right]_{+180}$ supercycle and a $90_0 - 360_{180} - 270_0$ C-element). The sum of double-quantum excitation and reconversion times was adjusted to $\tau_{DQ}^{total} = 2\,\text{ms}$ at a rotor spinning frequency of $\nu_r = 10\,\text{kHz}$. Different double-quantum conversion times τ_{DQ} can be realized by varying the number of C-elements of the reconversion/excitation blocks. From the acquired curves (see figure 9) distances were calculated by fitting simulated constant-time curves to the experimental ones. Numerically accurate simulations and the fitting procedures were done using SIMPSON [34, 35] with a powder average of 8584 orientations, with the dipolar-coupling constant and amplitude parameter as the only free fitting variables.

Double-quantum constant time experiments on **sample I** can be conducted without the need of an additional filter because it is isotopically labeled to a much lower degree than **sample II**. The pulse

sequence consists of two PostC7 blocks (as described above) to interconvert double-quantum and zero-quantum coherences (see figure 2, sequence C). Phase-cycling is identical to pulse-sequence A in figure 2 (see above), total conversion time $\tau_{DQ}^{total} = 2\,\mathrm{ms}$ and spinning-frequency $\nu_r = 10\,\mathrm{kHz}$.

2.4 DFT-Calculations

Density functional calculations of the proposed structures were done using GAUSSIAN 03 [36]. Geometries were optimized on a B3LYP/6-311++G** level of sophistication taking full advantage of the point group symmetry of each structure. Frequency calculations were performed for the smaller structures up to the octacyclo-α-pyrone to assure that the algorithm fell into a true minimum. The root mean deviation of the internuclear distance is expected to be below 0.017 Å [37]. Bond distances for infinite chains were approximated by calculating structures for fragments with 1 to 5 fused rings whose terminal bonds were saturated with hydrogen. The structures with five fused rings gave reasonably converged bond length values (< 0.01 Å) for the central ring carbon atoms.

3 Results and Discussion

3.1 Composition, Infrared Spectroscopy

Composition and IR spectra of the polymers obtained from polymerization in CCl_4 are in accordance with the results from previous work. Chemical analysis and IR spectroscopy, by the absence of bands in the CH-valence regime, indicate a very low content of hydrogen.

It is interesting to note that no two IR-spectra of poly(carbonsuboxide) in the literature are identical [9, 10, 13, 14]. This is a strong indication that from a preparative point of view experimental conditions strongly influence the structure of the polymer. There are however certain features in the IR-spectra which are observed throughout most of the literature reports. For samples which have not been in contact with moisture a band at $2171\,\mathrm{cm}^{-1}$ can be observed, which is attributed to a C=O bond vibration in ketene. Accordingly a sharp band at $530\,\mathrm{cm}^{-1}$ is caused by the C=C=O bending vibration (see figure 1). Haubenstock et al. [13] showed by combined IR/EPR experiments that these bands are probably caused by a ketenylfunction which is extremely sensitive to moisture.

The relative amount of ketenyl groups from IR alone is still unclear though. The IR spectra of our samples which had deliberately been exposed to air for 0, 2 and 5 s show that moisture extinguishes both ketene bands while a new band at 2336 cm^{-1} rises (see figure 1). We assign this new band to carbondioxide since similar values have been observed for CO_2 trapped in a solid matrix [2]. This interpretation is underlined by a second weak absorption at 2273 cm^{-1} which occurs for the air-exposed ^{13}C-labelled samples. This absorption corresponds to the asymmetric stretching mode of $^{13}CO_2$. In further agreement with this interpretation we find an additional band at 2125 cm^{-1} which is due to a ^{13}C=^{13}C=O ketenyl bending vibration. This indicates that ketenyl functions are oxidized on contact with air, forming carbondioxide which is trapped in the polymer matrix. Our results indicate that the absence of the ketene band in Paiaros [12] IR-spectra is a result of contact with moisture.

The most intensive bands in the IR-spectra appear between 1280 cm^{-1} and 1870 cm^{-1}. While it is difficult to draw conclusions about the structural background of these bands, it is reasonable to assume that at around 1800 cm^{-1} and at around 1500 cm^{-1} CO double bond vibrations and CC bond vibrations are the origin, respectively.

3.2 1D ^{13}C MAS NMR

We use ^{13}C solid-state MAS NMR to investigate the structure of solid poly(carbonsuboxide). The introduced isotopic labeling will allow us to study not only intensities and chemical shift but also ^{13}C-^{13}C distances and directly bonded neighbors, provided that ^{13}C-spectra have sufficient resolution and favorable relaxation properties.

The spectrum in figure 4 is representative for several batches of poly(carbonsuboxide) on which we did ^{13}C NMR. The resonance lineshapes allow to distinguish 4 main peaks at 96 ppm, 107.5 ppm, 150 ppm and 163 ppm which subsume to about 95% of the overall intensity. The spectrum was acquired using a rotor-synchronized spinecho experiment and a repetition delay ($> 5T_1$) which allows a meaningful analysis of the peak intensities. Spin-lattice relaxation times of the different resonances were determined from a saturation recovery experiment to be 765 s, 706 s, 706 s and 649 s on the **sample II**, respectively, while for the less intensive broad resonances also longer T_1-values of 1500 s are observed. The rather similar values of the main resonances are in accordance with car-

bons stemming from a single amorphous phase, where spin-diffusion would tend to even out major differences.

Since Haubenstock found that poly(carbonsuboxide) which had not been in contact with air is EPR active, we had to verify that we are able to get signals from all ^{13}C nuclei in the sample. To this end we mixed our sample with a known quantity of hexamethylbenzene, which gives 2 sharp NMR-resonances. From the mass we calculated the expected intensity ratio of the resonances of poly(carbonsuboxide) to those of hexamethylbenzene. The deviation is less than 5%. Apparently a strong coupling to unpaired electrons which would result in broadening and shifting of NMR resonances is not happening for most of the carbons in our samples. More important this indicates that EPR would allow only to investigate a very small portion of poly(carbonsuboxide). Additionally we have recorded IR spectra before and after the NMR experiment presented in figure 4 which gave almost identical IR spectra. The almost unchanged IR spectra including the intensive band at $2171\,\mathrm{cm}^{-1}$ of the very sensitive ketenyl function indicate that the material did not decompose throughout the NMR experiment.

Our main interest in the following is to assign the observed peaks to different structural motifs. Since in amorphous materials bond length and angles vary NMR-resonances are relatively broad. Still the observed resolution in the NMR spectra is impressive and the resonances resolve several distinct carbon environments. All observed chemical shifts lie in the region of sp/sp^2-hybridized carbon [38]. Since sp-hybridization can be excluded by absence of bands of $\mathrm{C} \equiv \mathrm{C}$ from the infrared spectrum, a structural model needs to be based on a trigonal-planar coordination environment for all carbon atoms.

In connection with the simple composition of poly(carbonsuboxide) this allows only for 3 different carbon environments in a one-bond sphere: carbon bonded to three other carbon atoms $\mathrm{C_{CCC}}$, carbon bonded to two carbon and one oxygen atom $\mathrm{C_{CCO}}$, carbon bonded to one carbon and two oxygen atoms $\mathrm{C_{COO}}$ and carbon bonded to three oxygen atoms $\mathrm{C_{OOO}}$. The carbonate environment $\mathrm{C_{OOO}}$ is very unlikely though, since ^{13}C double-quantum excitation via an INADEQUATE sequence for all observed peaks is possible (vide infra). Using isotropic chemical shift ranges in the literature [38] we assign the peaks at 96 ppm and 107.5 ppm to $\mathrm{C_{CCC}}$ and the peaks at 150 ppm and 163 ppm to $\mathrm{C_{CCO}}$ or $\mathrm{C_{COO}}$ environments. Clearly, for the low temperature polymerization route

chosen, the formation of carbon-rich oxygen-depleted areas with graphite like C_{CCC} environments can be ruled out by chemical shift arguments [39, 40]. The intensity ratio $\frac{I_{150\,\mathrm{ppm}}+I_{163\,\mathrm{ppm}}}{I_{96\,\mathrm{ppm}}+I_{107.5\,\mathrm{ppm}}}$ determined experimentally is approximately equal to 2 for **sample I** and 1 for **sample II**.

^{13}C-NMR spectra taken from samples which were carefully excluded from air and showed a strong ketene band in their IR spectra and ^{13}C NMR spectra of samples which were exposed for some seconds to air and did not show a ketene band in their IR were essentially identical. In other words, the strong ketene band from the IR spectra does not find its counterpart in the ^{13}C-NMR spectra, which indicates that the IR spectra are a very sensitive means of probing ketenyl functions while the relative amount in the samples is low.

3.3 The Polymerization Hypothesis

Underlying most of the older literature about "poly(carbonsuboxide)" and even its name is the chemically sensible assumption that the energetically expensive monomer C_3O_2 on polymerization is forming additional CO and CC bonds which finally form a 2D polymer. This assumption has important implications for both the reaction mechanism and possible polymer structures. In the light of a highly unsaturated carbon species which might also undergo a sigmatropic rearrangements it is necessary to question the CC bond conservation throughout the reaction and with it the polymerization hypothesis.

In case of **sample I** we have the ideal test candidate to answer the questions if CC bonds are conserved by the reaction or not. The educts of **sample I** consist of triply labeled $^{13}C_3 - C_3O_2$ diluted in C_3O_2 at natural abundance of the isotopes. If the reaction pathway is a simple polymerization lacking sigmatropic rearrangements we would expect clusters of three NMR active spin-1/2 nuclei while bond breaking would make clusters of maximum two spin-1/2 nuclei much more likely. There is a range of solid-state high-resolution NMR techniques to solve this problem. Examples are spin-counting experiments [41] and experiments making use of the special properties of the top-quantum in an n-spin-1/2 system [42]. In this simple case the most straightforward approach is probably the excitation of triple-quantum coherences for which three spin-1/2 nuclei are necessary. Furthermore if triple-quantum coherences are excited via through-bond dipolar coupling for short excitation times than the three spin-1/2 nuclei have to be directly bonded. We have used a rotor-synchronized

2D triple-quantum MAS correlation experiment based on the INADEQUATE experiment (see figure 2, pulse-sequence B) to resolve possibly overlapping peaks. The triple-quantum 2D spectrum in figure 7 shows several peaks to which all carbon behind the main peaks contribute. Hence the triple-quantum spectrum strongly indicates that the CC-bonds of the monomer are conserved throughout the reaction. An explanation for the absence of the peaks at 150 ppm and 163 ppm in the 2D triple-quantum spectrum is straight forward [1]. Information about the coupling partners of the nucleus behind the observed triple-quantum filtered resonance can be reconstructed from the observed resonance frequencies in the indirect dimension. The triple-quantum coherence is evolving under the sum of the chemical shifts of the contributing spins in the indirect dimension, meaning that the resonance frequencies can be predicted from the 1D spectrum. The peaks were marked A, B, C, D for this purpose and the peaks contributing to each triple-quantum peak designated in the spectrum (see figure 7). We will return to the triple-quantum spectrum after the assignment of the peaks using double-quantum techniques and discuss the spectrum in more detail then.

3.4 Further Assignment of ^{13}C NMR Peaks by 2D Methods

After confirmation of the polymerization hypothesis we study how C_3O_2 monomers are linked in the polymer using double-quantum NMR. In homonuclear ^{13}C double-quantum filtered NMR only pairs of ^{13}C atoms give rise to signals, all isolated ^{13}C nuclei are filtered out. If again the through-bond coupling between ^{13}C-nuclei is used for multiple-quantum coherence excitation only directly

[1] The spin-system of the three nuclei from $^{13}C_3 - C_3O_2$ after polymerization will be isolated from the next nearest ^{13}C spins for statistical reasons. The spin-system of these three nuclei will be linear in the sense that only one carbon atom is directly bound to the two others. In terms of J couplings this means that the middle spin will have two strong ^1J couplings in the range of 40 to 100 Hz magnitude while the other two spins are strongly coupled only to the middle spin and have a weak ^2J coupling to the not directly bonded carbon. In an amorphous material it is very likely that all three spins are not isochronous due to variations in the chemical shift by variations in their chemical surrounding. This separation for almost all nuclei will be sufficient to put the three spin system into the weak coupling limit [43,44]. Under these conditions the evolution of the spin system and hence the peak intensities of the 2D triple-quantum spectrum can be analyzed with the product operator formalism. The conversion mechanism between triple-quantum coherences and zero-quantum coherences becomes significantly simplified by the fact that the contribution of the three J couplings to the Hamiltonian commute with each other in the weak coupling limit. As a result the triple-quantum filtered efficiency A of a nucleus i only depends on the J couplings J_{ij} and J_{ik} but not on J_{jk} upon variation of the triple-quantum reconversion time τ_{TQ}^{reconv}.

$$A_i \propto -\cos\left[\pi\,(J_{ij}-J_{ik})\,\tau_{TQ}^{reconv}\right] + \cos\left[\pi\,(J_{ij}+J_{ik})\,\tau_{TQ}^{reconv}\right]$$

For the limiting case where the two-bond J coupling constant is zero only the middle spin can be observed. This is exactly what is observed in the experimental triple-quantum 2D spectrum in figure 7.

bonded neighbors will be observed. For **sample II** which was made from a mixture of $O=C^*=C=C^*=O$, $O=C=C^*=C=O$ and C_3O_2 at natural abundance, this means that every double-quantum filtered signal represents a bond between 2 different monomers.

As triple-quantum NMR indicates that CC bonds of the monomer are conserved, it follows that only the environments C_{CCC} and C_{CCO} will be able to pass the double-quantum filter, the carbon in the C_{COO} environment is only bound to a carbon atom of the same monomer which, by the labeling scheme applied, is suppressed through the double-quantum filter. Based on the above considerations the 2D double-quantum filtered correlation spectrum in figure 6 allows a clear assignment of the peaks at 150 ppm and 163 ppm. Only the resonance at 163 ppm gives double-quantum coherence peaks with the resonances at 96 ppm and 107.5 ppm representing a C_{CCC} carbon atom, hence the peak at 163 ppm represents a C_{CCO} carbon atom and the peak at 150 ppm C_{COO} carbon.

3.5 Intramonomeric and Intermonomeric Short-Range Order

After assignment of the peaks it is interesting to explore the direct surrounding of the carbons behind these resonances. Double-quantum filtered 2D correlation spectra give correlation signals for every carbon atom pair in neighboring environments. In principle the following six pairs are possible $\langle C_{CCC}-C_{CCC}\rangle$, $\langle C_{CCC}-C_{CCO}\rangle$, $\langle C_{CCC}-C_{COO}\rangle$, $\langle C_{CCO}-C_{CCO}\rangle$, $\langle C_{CCO}-C_{COO}\rangle$ and $\langle C_{COO}-C_{COO}\rangle$. The intramonomeric arrangement becomes obvious in the 2D correlation of **sample I** (see figure 5). Only double-quantum correlation signals for the pairs $\langle C_{CCC}-C_{CCO}\rangle$ and $\langle C_{CCC}-C_{COO}\rangle$ are visible. This is a remarkable result because it suggests that amorphous $(C_3O_2)_x$ has a well defined short range order. Finally using triple-quantum filtered 2D correlation spectroscopy of **sample I** the terminal positions of the polymerized C_3O_2 can be determined. In the triple-quantum correlation spectrum two signals for the C_{CCC} carbons at 96 ppm (peak D) and 107.5 ppm (peak C) are visible with a distribution of chemical shifts in the indirect dimension with a double maximum each. These maxima in the indirect dimension of peaks C and D are identified as belonging to triple-quantum coherence with peaks A and B and with peaks A and A. As the spread in isotropic chemical shift for C_{CCO} and C_{CCC} carbon atoms is small (see 2D spectrum in figure 7) this is indicative of a rather wide chemical shift distribution for carbon in the C_{COO} environment with 2 maxima one at 150 ppm and one at 163 ppm, which also explains for the intensity distribution

found in the quantitative 1D spectrum. In a simple model with 3 distinct environments for C_{CCC}, C_{CCO} and C_{COO} carbons an intensity ratio for **sample I** of 1:1:1 would be expected which clearly is not the case. Consequently the combined double-quantum and triple-quantum 2D results on **sample I** are best interpreted as two types of $^{13}C-{}^{13}C-{}^{13}C$ units consisting of $C_{CCO}-C_{CCC}-C_{COO}$ triples, with two different C_{CCC} carbons to explain for the signals at 96 ppm and 107.5 ppm and a rather wide distribution of isotropic chemical shifts for the C_{COO} carbon from 150 ppm to 163 ppm and one type of environment for the C_{CCO} carbon at 163 ppm.

The intermonomeric connectivity is determined from double-quantum filtered experiments of **sample II**. Double-quantum excitation can be achieved with two complementary types of experiments. While experiments using the through-bond dipolar interaction give clear results with respect to the chemically bound neighbors, experiments based on the through-space dipolar interaction allow to probe the spatial vicinity of an NMR active nucleus. Besides, through-space dipolar coupling based experiment give access to internuclear distance. So far we have only made use of through-bond coupling based 2D correlation experiments. For the intermonomeric connectivity there are only three possibilities: $\langle C_{CCC}-C_{CCC}\rangle$, $\langle C_{CCC}-C_{CCO}\rangle$, $\langle C_{CCO}-C_{CCO}\rangle$. The J coupling based double-quantum spectrum of **sample II** (see figure 6) shows even to very low levels of intensity signals of double-quantum coherences for $\langle C_{CCC}-C_{CCO}\rangle$ carbon pairs only, the to be expected signals for other possibilities are not observed. Comparing a double-quantum through-space 2D correlation spectrum of **sample II** (see figure 8) the same peaks as in the through-bond version can be found. Extra correlation signals for coherences of $\langle C_{CCC}-C_{CCC}\rangle$ and $\langle C_{CCO}-C_{CCO}\rangle$ carbon pairs are present. From the appearance of a $\langle C_{CCC}-C_{CCC}\rangle$ double-quantum coherence between the peaks at 96 ppm and 107.5 ppm it may be concluded that both environments occur in spatial proximity and from the relative peak intensities of the double-quantum coherence signals $\left\langle C_{CCC}^{96\,\mathrm{ppm}}-C_{CCC}^{96\,\mathrm{ppm}}\right\rangle$, $\left\langle C_{CCC}^{96\,\mathrm{ppm}}-C_{CCC}^{107.5\,\mathrm{ppm}}\right\rangle$ and $\left\langle C_{CCC}^{107.5\,\mathrm{ppm}}-C_{CCC}^{107.5\,\mathrm{ppm}}\right\rangle$ that the proximity of equal pairs is more likely.

3.6 More Structural Constraints: $C-C$ Distances by Double-Quantum Constant-Time Double-Filtering Experiments

Internuclear distances can give important constraints even in amorphous materials. It is well know from analysis of crystallographic databases that $C-C$ distances [45] often vary only in a very narrow range for a given pair of carbon functions. Recently internuclear distances determined by ^{13}C double-quantum NMR have been shown to be accurate enough to differentiate between single, double, and triple bonds of carbon atoms [25]. In order to obtain further constraints to refine the structural model of poly(carbonsuboxide) we have determined approximate values for carbon-carbon distances from dipolar oscillations in double-quantum constant-time build-up curves [24]. Since distance determination by ^{13}C double-quantum solid-state NMR requires dilute $^{13}C-^{13}C$ spin-pairs, distance constraints could only be obtained from **sample II**. We have acquired double-filtering double-quantum constant-time build-up curves for both $C_{CCC}-C_{CCO}$ intermonomeric double-quantum signals for the signals at 107.5 ppm and 96 ppm (see figure 9). The experimental curves were fitted with only two free variables, one for the dipolar coupling constant and one for the amplitude. The $C-C$ distances for the $C_{CCO}^{163\,ppm}-C_{CCC}^{107.5\,ppm}$ and the $C_{CCO}^{163\,ppm}-C_{CCC}^{96\,ppm}$ pairs were 1.42 ± 0.03 Å and 1.41 ± 0.03 Å, respectively.

Distances may structurally be interpreted with the help of empiric bond length distribution parameters like mean and the lower and upper quartile which are available for many structural fragments via the Cambridge Structural Database. In figure 10 the distribution parameters of carbon-carbon bond lengths for various functional groups are presented which have been determined from a huge number of crystal structure determinations. The distributions of bond length are partially well separated: Unconjugated double and single $C-C$ bonds can easily be distinguished, but also with increasing bond order the distances of conjugated single-bonds show a difference between heterocycles like α-pyrone and furan structures and chain-like structures like in conjugated alkenes. Comparing experimental values with the empirical distance distribution we conclude that $C-C$ bonds of a bond-order below 1.5 in α-pyrone and furan like structures best describe the experimental results.

3.7 Structural Models

In the literature the structural models discussed for poly(carbonsuboxide) are manifold. Even in the more recent literature there have been new propositions [12,19]. Definitely the first ideas of Diels are not consistent with many experimental facts which have been gathered over the years. We require models to consist of sp^2-hybridized carbon with an average composition equal to the monomer C_3O_2. Minor contributions like ketene functions which are probably associated with the terminal positions of the polymer will not be considered. Furthermore we require the structural models to be a hypothetical product of a polymerization, i. e. $C-C$ bonds of the monomer are conserved. While solid-state NMR provides indirect information about the polymerization mechanism, we consider an in-depth discussion of the mechanism futile as long as it is not clear whether it takes a radical or an ionic path. Haubenstocks investigations, however, indicate a non-radical mechanism [13].

In figure 11 a collection of structural models is compiled. All of the model structures consist of either α-pyrone or γ-pyrone units which are arranged in cyclic or chain like fashion. Bond distances were estimated from DFT calculations (see table 1). The effects of the ring-strain and conjugation are apparent from the gradual change in bond lengths of the two types of C_{CCC}-C_{CCO} bonds. While in cyclohexa-α-pyrone C_{CCC}-C_{CCO} bonds can still be described as localized double- and single-bonds, for the planar poly-α-pyrone the roles are interchanged and bond lengths are almost equal.

After these general remarks we will discuss the individual models with respect to the NMR results in detail. Besides chemical shift, composition and relative proportions of the ^{13}C peak intensities we will make use of the connectivity patterns observed in the 2D experiments and the associated distances. To this end we need to have an idea which carbon atoms in the polymer formerly belonged to the same monomer. The assignment is based on the arrangement of the "terminal" C_{COO} carbon atoms. The monomer units are highlighted in figure 11 by the use of bold type. With the exception of the α-pryone structures A and C the assignment is unique.

The anti-catena-γ-pyrone (model E in figure 11) is clearly not a good description of poly(carbonsuboxide) because C_{CCC} carbon atoms are not present in its structure hence the NMR peaks at 107.5 ppm and 96 ppm cannot be explained. Moreover there are only two substantially different carbon environments which both take part in an intermonomeric bonding, which contradicts the double-quantum 2D correlation experiments on **sample II**. The same chain of reasons rule out a

cyclo-hexa-γ-pyronic structure (model B in figure 11).

The syn-catena-γ-pyrone (model F in figure 11) is a better choice with respect to the number of carbon environments and their expected isotropic chemical shifts. It fullfills the requirement of one terminal carbon atom C_{COO} linked to a C_{CCC} carbon atom which in turn is bound to a C_{CCO} carbon atom. However the expected intermonomeric C_{CCC}-C_{CCO} bond length of 1.50 Å does not agree with the experimental value of 1.42 Å or 1.41 Å, which makes model F rather unlikely.

For the iso-catena-poly-α-pyrone (model D in figure 11) three types of carbon atom environments C_{COO}, C_{CCC}, C_{CCO} would be expected. The intramonomeric bonding C_{COO}-C_{CCC}-C_{CCO} complies with the double-quantum spectra of **sample I** but the intermonomeric bond does not. In fact strong intermonomeric $C_{CCC} - C_{CCC}$ and $C_{CCO} - C_{CCO}$ double-quantum coherences on **sample II** would be expected which is not the case.

For catena-α-pyrone (model C in figure 11) three carbon environments C_{COO}, C_{CCC}, C_{CCO} are expected. Connectivity patterns in the double-quantum correlation spectra of **sample I** and **II** and the expected chemical shifts are in excellent agreement with the structural model, no matter how the assignment, which carbons belong to the same monomer, is done. The same is true for the closely related cyclo-α-pyrone structures. Again the intermonomeric $C - C$ distance can be used to get further insight. The values for the intermonomeric bond length disagree with the cyclo-hexa-α-pyronic structure while the bigger sized rings and the planar poly-α-pyrone give reasonable values.

^{13}C MAS NMR of poly(carbonsuboxide) resolves two peaks for the C_{CCC} environment. Both carbon environments are present in the NMR spectra of several batches while their relative peak intensities vary. An explanation might be that in the amorphous solid $(C_3O_2)_x$ planar and bent structures coexist - possibly even in cyclic arrangements.

4 Conclusions

In contrast to previous studies of poly(carbonsuboxide) we have reported by the use of ^{13}C solid-state NMR the first quantitative investigation of the bulk structure of poly(carbonsuboxide). By the use of chemical shift arguments and the combination of selective labeling with 2D double-quantum correlation spectroscopy it was possible to assign the observed peaks in the ^{13}C NMR spectrum to

different carbon environments. On the methodological side it was shown that distance-determination by ^{13}C double-quantum NMR can be applied to heavily labeled materials by the use of double-filtering methods. The determined CC bond lengths were analyzed with the help of empirical bond length distribution parameters for various functional groups extracted from the Cambridge Structural Database. Propositions for the local structure of poly(carbonsuboxide) were collected. Their CC bond length values were predicted with the help of DFT-calculations. Based on the presented arguments it was possible to evaluate different structural models. Our results unambiguously rule out poly-γ-pyronic structural models recently proposed in the literature [12]. Our results are in agreement with the poly-α-pyronic structures discussed by several other authors [7–10, 13, 17, 18, 20]. In addition our results give constraints for the polymerization mechanism and some indications about the possibility of cyclic and planar polymeric structures. Still some aspects are not fully understood. For example the ^{13}C MAS NMR spectrum resolves two different alkene carbons and IR spectra in several published articles significantly differ for unknown reasons. We conclude that despite the almost 100 years of chemical history of poly(carbonsuboxide) there are still many open questions to be answered.

5 Acknowledgments

Support within the collaborative research center (SFB408) by the Deutsche Forschungsgemeinschaft is gratefully acknowledged. In the framework of the "Rechenverbund-NRW" we would like acknowledge the usage of the computing center of the RWTH Aachen. For many discussions and comments on the DFT calculations we would like to thank G. von Frantzius and B. A. Hess. We are grateful to G. Dittmann for assistance in the synthesis of the labeled compounds and M. Koch, B. Knopp, and V. Bendisch for specimen preparation and recording of the IR spectra.

References

[1] O. Diels and B. Wolf, *Ber. Deut. Chem. Gesell.*, 1906, **39**, 689–697.

[2] P. A. Gerakines and M. H. Moore, *Icarus*, 2001, **154**, 372–380.

[3] M. N. Fomenkova, *Space Sci. Rev.*, 1999, **90**, 109–114.

[4] R. Grauer, *Chimia*, 1960, **14**, 11–16.

[5] A. Ellern, T. Drews, and K. Seppelt, *Z. Anorg. Allg. Chem.*, 2001, **627**, 73–76.

[6] L. Birkhover and P. Sommer, *Chem. Ber.*, 1976, **109**, 1701–1707.

[7] N. L. Yang, A. Snow, H. Haubenstock, and F. Bramwell, *J. Polym. Sci.*, 1978, **16**, 1909–1927.

[8] A. R. Blake, W. T. Eeles, and P. P. Jennings, *Trans. Faraday Soc.*, 1964, **60**, 691–699.

[9] R. N. Smith, D. A. Young, E. N. Smith, and C. C. Carter, *Inorg. Chem.*, 1963, **2**, 829–838.

[10] A. R. Blake, W. T. Eeles, and P. P. Jennings, *Trans. Faraday Soc.*, 1964, **60**, 1775–1782.

[11] I. M. Barkalov, I. P. Kim, A. I. Mikhailov, and D. P. Kiryukhin, *J. Polym. Sci.: Polym. Chem. Ed.*, 1980, **18**, 1551–1558.

[12] T. Carofiglio, L. Pandolfo, and G. Paiaro, *Eur. Polym. J.*, 1986, **22**, 491–497.

[13] A. W. Snow, H. Haubenstock, and N. L. Yang, *Macromolecules*, 1978, **11**, 77–86.

[14] L. Schmidt, H.-P. Boehm, and U. Hofmann, *Z. Anorg. Allg. Chem.*, 1958, **296**, 246–261.

[15] O. Diels and G. Meyerheim, *Ber. Deut. Chem. Gesell.*, 1907, **40**, 355–363.

[16] B. D. Kybett, G. K. Johnson, C. K. Barker, and J. L. Margrave, *J. Phys. Chem.*, 1965, **69**, 3603–3606.

[17] A. R. Blake, *J. Chem. Soc.*, 1965, pp. 3866–3867.

[18] N.-L. Yang, A. Snow, and H. Haubenstock, *Am. Chem. Soc., Div. Polym. Chem.*, 1981, **22**, 52–53.

[19] F. Kerek Bundesrepublik Deutschland, Deutsches Patent- und Markenamt, DE 19600301 C2, 1999.

[20] E. Ziegler, *Angew. Chem.*, 1960, **72**, 582.

[21] M. Ballauff, L. Li, S. Rosenfeldt, N. Dingenouts, J. Beck, and P. Krieger-Beck, *Angew. Chem., Int. Ed.*, 2004, **43**, 5843–5846.

[22] H. Eckert, *NMR Basic Princ. Prog.*, 1994, **33**, 125–198.

[23] S. P. Brown and H. W. Spiess, *Chem. Rev.*, 2001, **101**, 4125–4155.

[24] J. Schmedt auf der Günne, *J. Magn. Reson.*, 2003, **165**, 18–32.

[25] M. Carravetta, M. Edén, O. G. Johannessen, H. Luthman, P. J. E. Verdegem, J. Lugtenburg, A. Sebald, and M. H. Levitt, *J. Amer. Chem. Soc.*, 2001, **123**, 10628–10638.

[26] P. E. Kristiansen, M. Carravetta, W. C. Lai, and M. H. Levitt, *Chem. Phys. Lett.*, 2004, **390**, 1–7.

[27] S. Kiihne, K. B. Geahigan, N. A. Oyler, H. Zebroski, M. A. Mehta, and G. P. Drobny, *J. Phys. Chem.*, 1999, **A103**, 3890–3903.

[28] E. A. Williams, J. D. Cargioli, and A. Ewo, *Chem. Comm.*, 1975, pp. 366–367.

[29] A. Lesage, C. Auger, S. Caldarelli, and L. Emsley, *J. Amer. Chem. Soc.*, 1997, **119**, 7867–7868.

[30] D. J. States, R. A. Haberkorn, and D. J. Ruben, *J. Magn. Reson.*, 1982, **48**, 286–292.

[31] M. H. Levitt, P. K. Madhu, and C. E. Hughes, *J. Magn. Reson.*, 2002, **155**, 300–306.

[32] K. Saalwächter, P. Ziegler, O. Spyckerelle, B. Haidar, A. Vidal, and J.-U. Sommer, *J. Chem. Phys.*, 2003, **119**, 3468–3482.

[33] M. Hohwy, H. J. Jakobsen, M. Edén, M. H. Levitt, and N. C. Nielsen, *J. Chem. Phys.*, 1998, **108**, 2686–2694.

[34] M. Bak, J. T. Rasmussen, and N. C. Nielsen, *J. Magn. Reson.*, 2000, **147**, 296–330.

[35] T. Vosegaard, A. Malmendal, and N. C. Nielsen, *Monatsh. Chem.*, 2002, **133**, 1555–1574.

[36] M. J. Frisch, G. W. Trucks, H. B. Schlegel, G. E. Scuseria, M. A. Robb, J. R. Cheeseman, J. A. Montgomery, T. Vreven, K. N. Kudin, J. C. Burant, J. M. Millam, S. S. Iyengar, J. Tomasi, V. Barone, B. Mennucci, M. Cossi, G. Scalmani, N. Rega, G. A. Petersson, H. Nakatsuji, M. Hada, M. Ehara, K. Toyota, R. Fukuda, J. Hasegawa, M. Ishida, T. Nakajima, Y. Honda, O. Kitao, H. Nakai, M. Klene, X. Li, J. E. Knox, H. P. Hratchian, J. P. Cross, C. Adamo, J. Jaramillo, R. Gomperts, R. E. Stratmann, O. Yazyev, A. J. Austin, R. Cammi, C. Pomelli, J. W. Ochterski, P. Y. Ayala, K. Morokuma, G. A. Voth, P. Salvador, J. J. Dannenberg, V. G. Zakrzewski, S. Dapprich, A. D. Daniels, M. C. Strain, O. Farkas, D. K. Malick, A. D. Rabuck, K. Raghavachari, J. B. Foresman, J. V. Ortiz, Q. Cui, A. G. Baboul, S. Clifford, J. Cioslowski, B. B. Stefanov, G. Liu, A. Liashenko, P. Piskorz, I. Komaromi, R. L. Martin, D. J. Fox, T. Keith, M. A. Al-Laham, C. Y. Peng, A. Nanayakkara, M. Challacombe, P. M. W. Gill, B. Johnson, W. Chen, M. W. Wong, C. Gonzalez, and J. A. Pople, Gaussian, Inc., Pittsburgh PA, 2003.

[37] D. Young, Wiley Interscience, 2001.

[38] M. Hesse, H. Meier, and B. Zeeh, Thieme, 1991.

[39] C. Goze-Bac, S. Latil, P. Lauginie, V. Jourdain, J. Conard, L. Duclaux, A. Rubio, and P. Bernier, *Carbon*, 2002, **40**, 1825–1842.

[40] T. M. Alam, T. A. Friedmann, P. A. Schultz, and D. Sebastiani, *Phys. Rev. B*, 2003, **67**, 245309–1–245309–11.

[41] N. A. Oyler and R. Tycko, *J. Phys. Chem. B*, 2002, **106**, 8382–8389.

[42] C. E. Hughes, J. Schmedt auf der Günne, and M. H. Levitt, *Chem. Phys. Chem.*, 2003, **4**, 457–465.

[43] M. H. Levitt, Wiley, 2001.

[44] R. R. Ernst, G. Bodenhausen, and A. Wokaun, International Series of Monographs on Chemistry, Oxford University Press, 1987.

[45] F. H. Allen, O. Kennard, D. G. Watson, L. Brammer, G. Orpen, and R. Taylor, *J. Chem. Soc. Perkin Trans.*, 1987, **II**, S1–S19.

Table 1: bond lengths d for inter- and intramonomeric $C_{CCC} - C_{CCO}$ bonds calculated by quantum-mechanical methods; the letters in the second column refer to the structures in figure 11.

Structure		$d^{\text{inter}}/\text{Å}$	$d^{\text{intra}}/\text{Å}$
cyclo-hexa-α-pyrone	A, [19]	1.359	1.473
cyclo-octa-α-pyrone	[19]	1.397	1.428
cyclo-deca-α-pyrone	[19]	1.407	1.416
cyclo-dodeca-α-pyrone	[19]	1.419	1.402
catena-poly-α-pyrone	C, [20]	1.437	1.392
iso-catena-poly-α-pyrone	D	-	1.432
cyclo-hexa-γ-pyrone	B, [19]	-	-
anti-catena-poly-γ-pyrone	E, [12]	-	-
syn-catena-poly-γ-pyrone	F, [12]	1.500	1.500

List of Figures

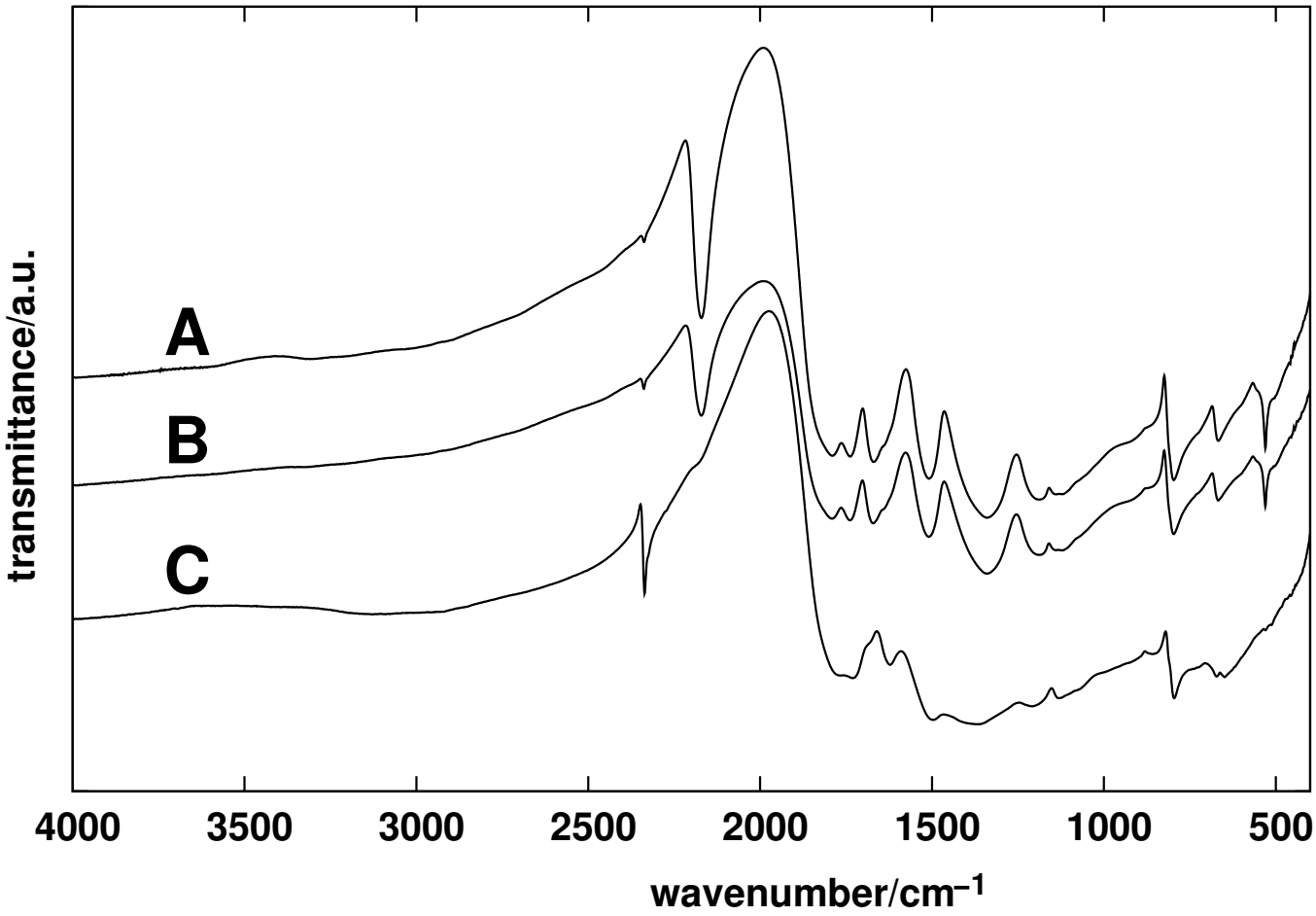

Figure 1: Infrared spectra of poly(carbonsuboxide) whose isotopes are at natural abundance; spectrum A refers to a sample which has not been exposed to air, spectrum B and C to a sample from the same charge which have been exposed to air for 2 s and 5 s, respectively.

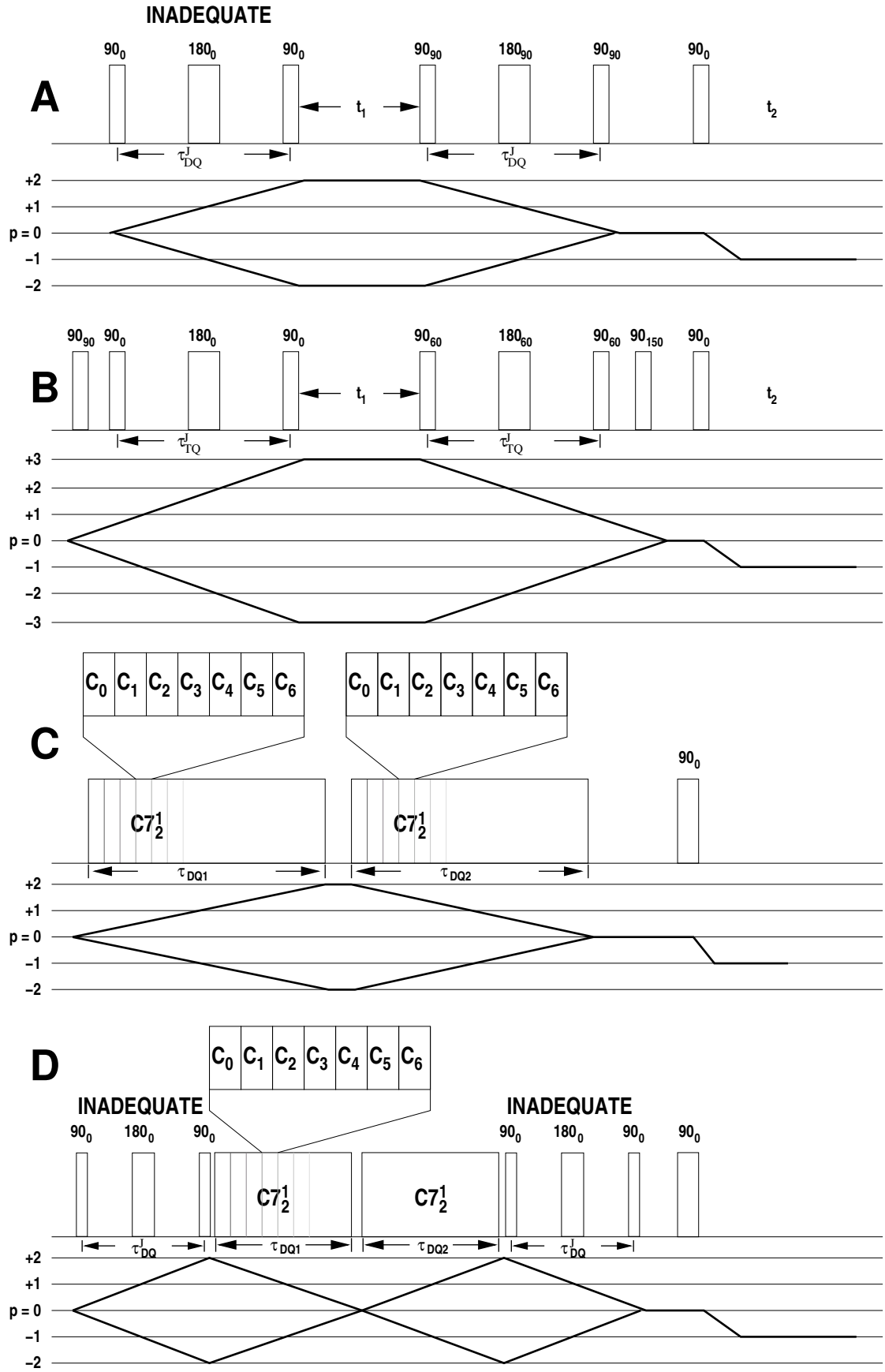

Figure 2: Multiple-quantum pulse sequences (schematic); pulse-sequences A and B were used for through-bond double-quantum filtered 2D experiments; pulse-sequences C and D for acquisition of constant-time double-quantum build-up curves; the pulses during the INADEQUATE blocks are rotor-synchronized, in the sense that the delay between the gravity of the pulses coincides with a multiple of a full rotor period; active rotor-synchronization on a trigger-signal from the probe is recommended in case of long τ^J_{DQ} delays.

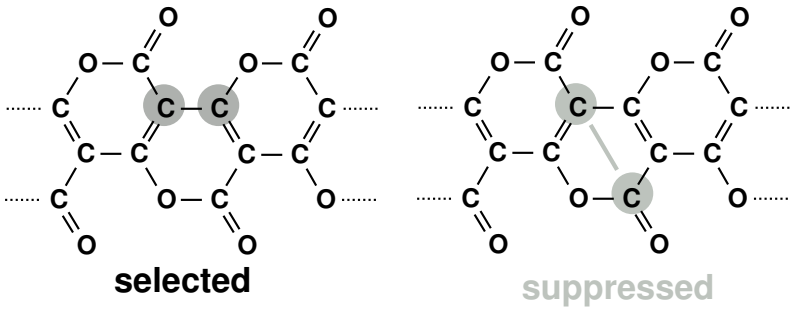

Figure 3: ^{13}C-^{13}C spin-pairs selected and suppressed by ^{13}C double-quantum double-filtering NMR; the underlying grey circles mark ^{13}C nuclei; only spin-pairs connected over a CC bond contribute to the double-quantum filtered signal; the spin-pair shown on the right hand side has negligible J coupling and is filtered out.

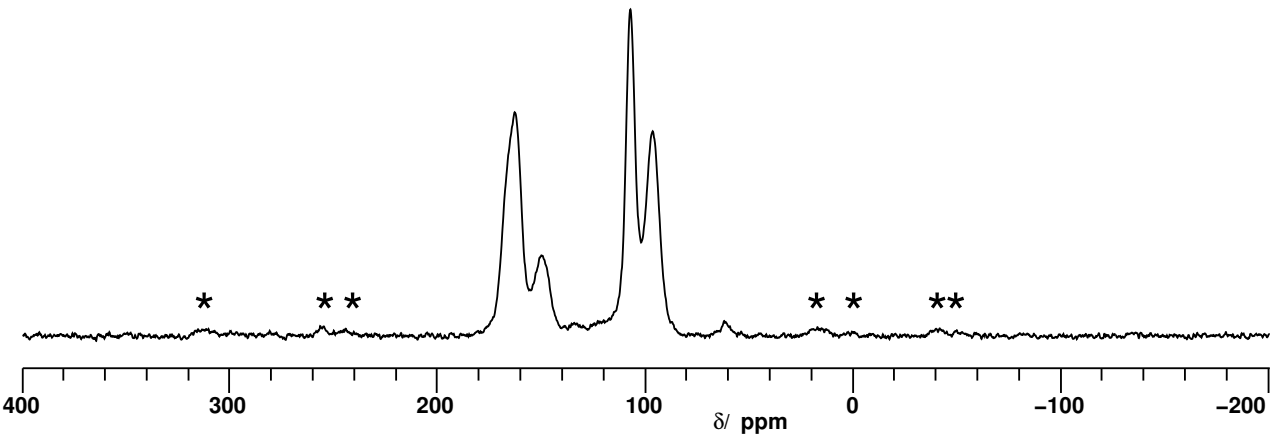

Figure 4: 1D ^{13}C MAS NMR spectra of polycarbonsuboxide (**sample II**); spinning sidebands are marked with an asterisk, $\nu_r = 15\,\mathrm{kHz}$, repetition rate 9000 s.

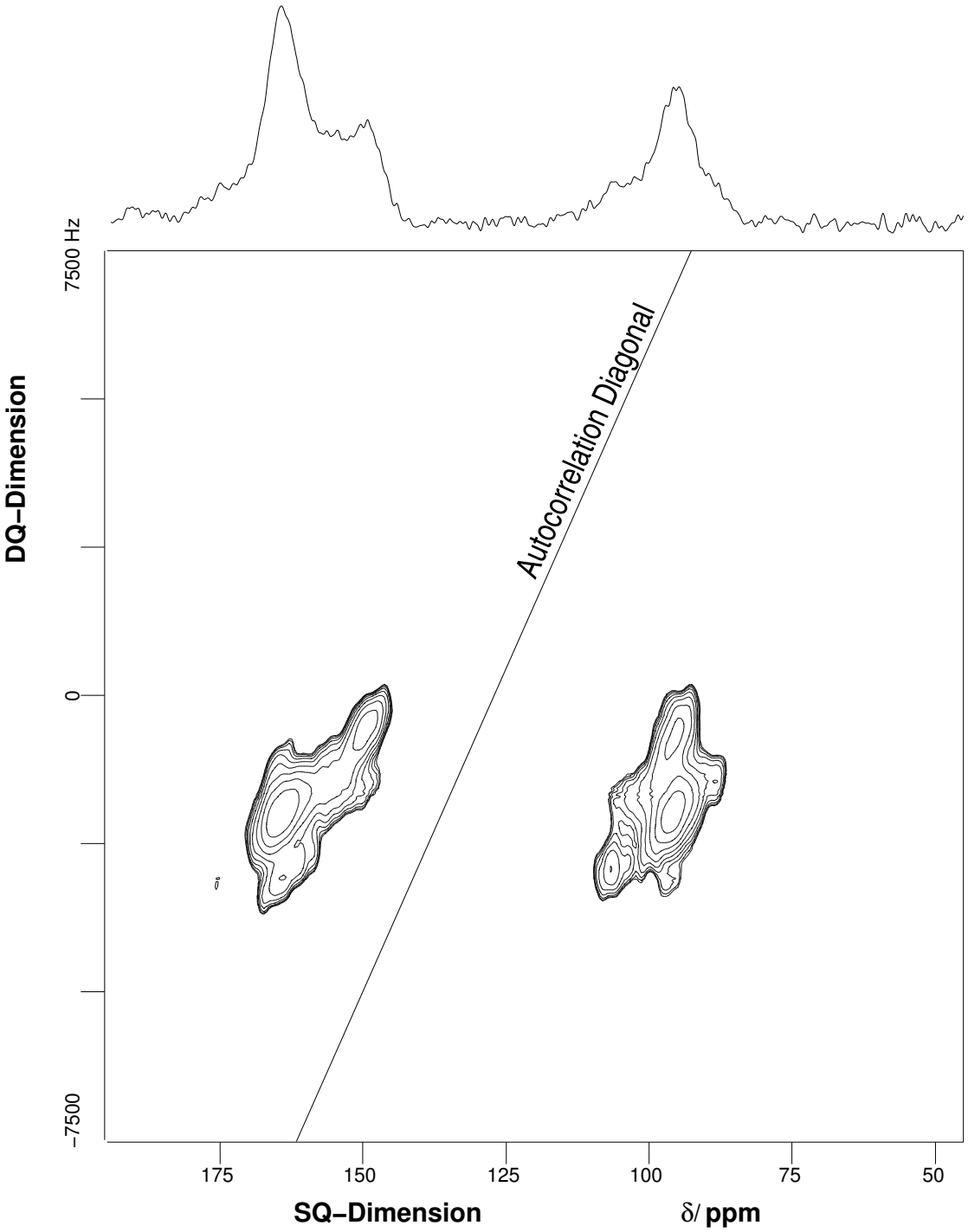

Figure 5: 2D double-quantum filtered correlation spectrum of polycarbonsuboxide (**sample I**) using the through-space dipolar coupling; the double-quantum/zero-quantum conversion times τ_{DQ} with 1.067 ms are short enough to ensure that the double-quantum peak intensities reflect directly bound CC pairs.

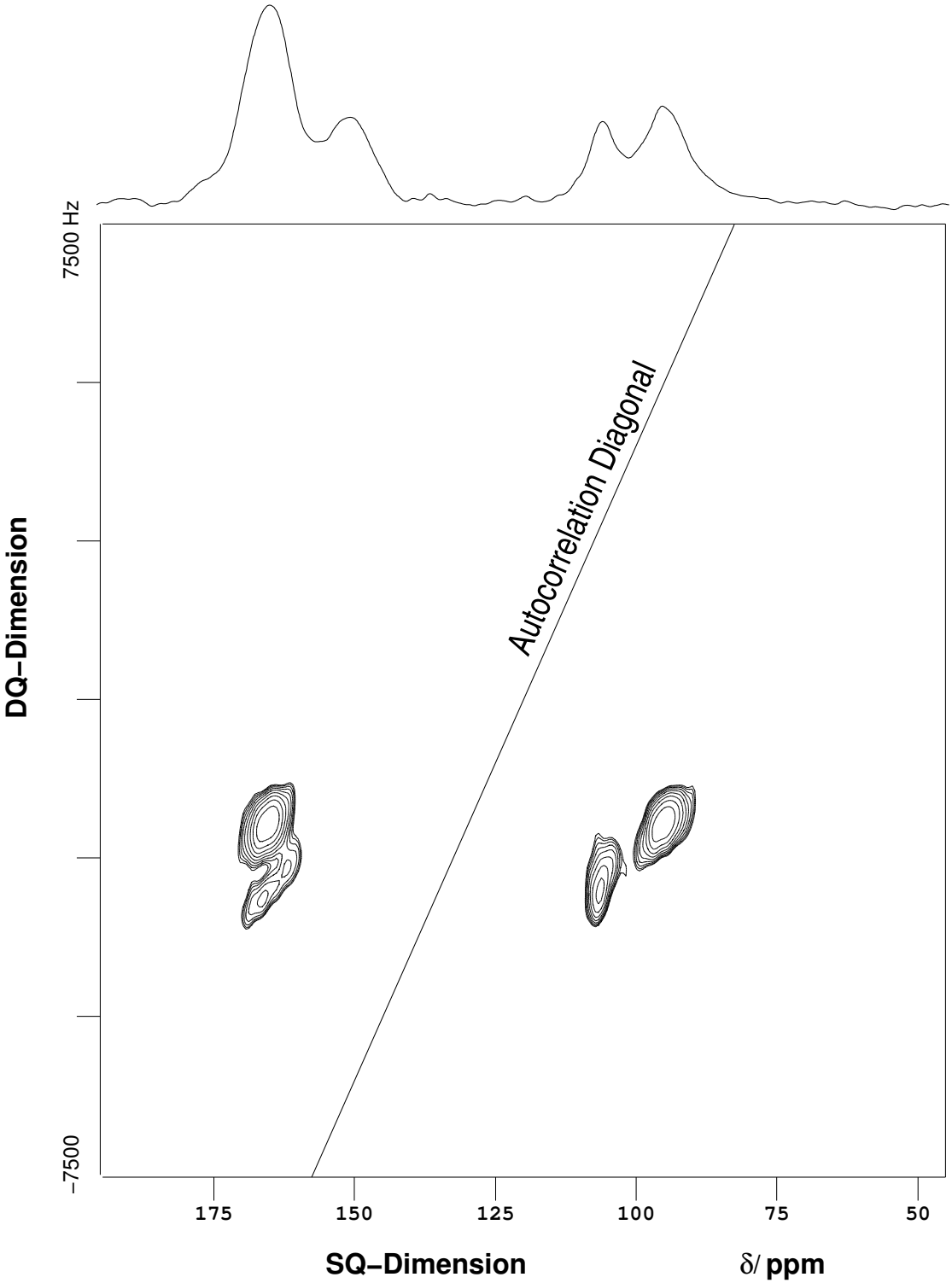

Figure 6: 2D double-quantum filtered correlation spectrum of poly(carbonsuboxide) (**sample II**) using the through-bond dipolar coupling for double-quantum coherence excitation (pulse-sequence A, figure 2).

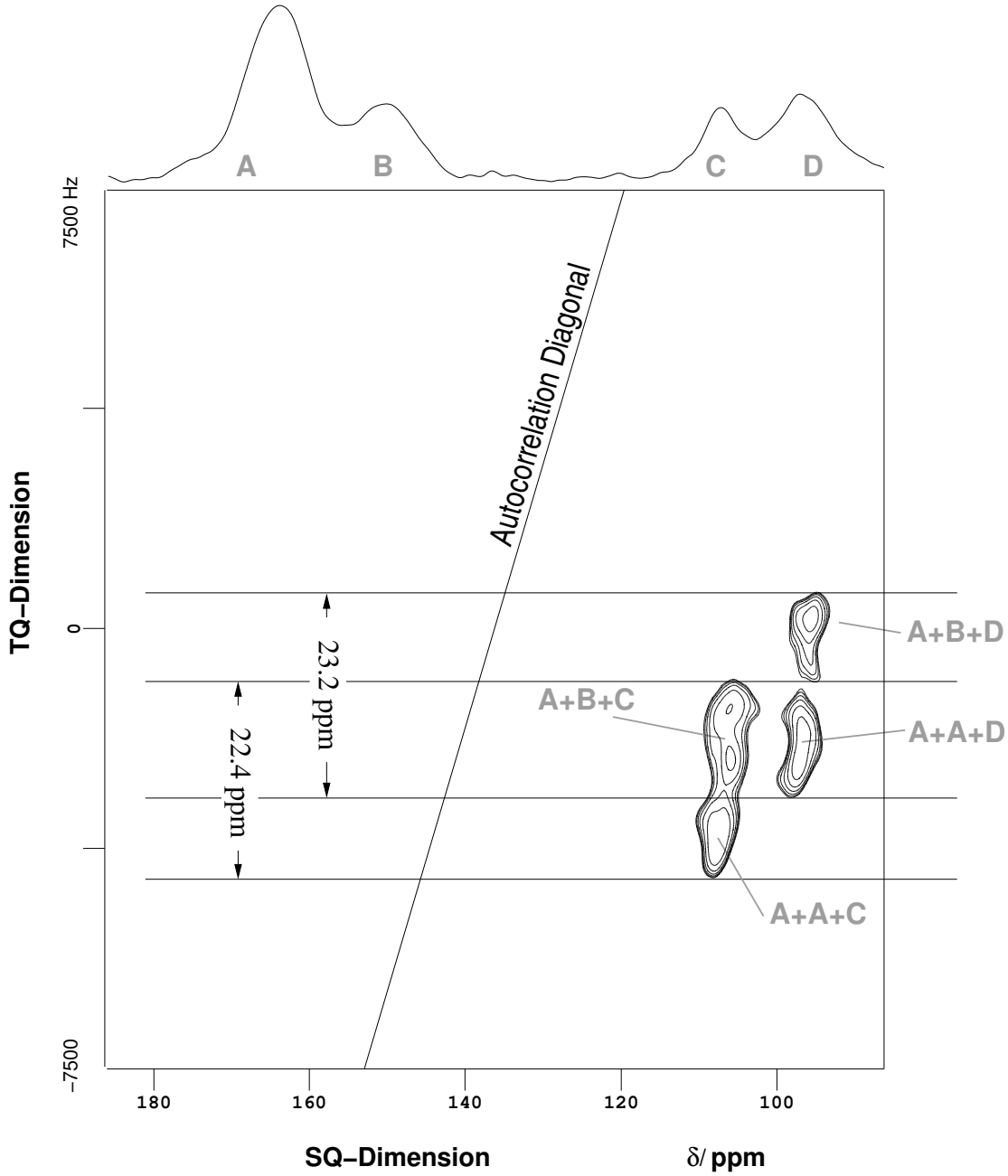

Figure 7: 2D triple-quantum filtered correlation spectrum of poly(carbonsuboxide) (**sample I**) using the through-bond dipolar coupling for triple-quantum coherence excitation (pulse-sequence B, figure 2).

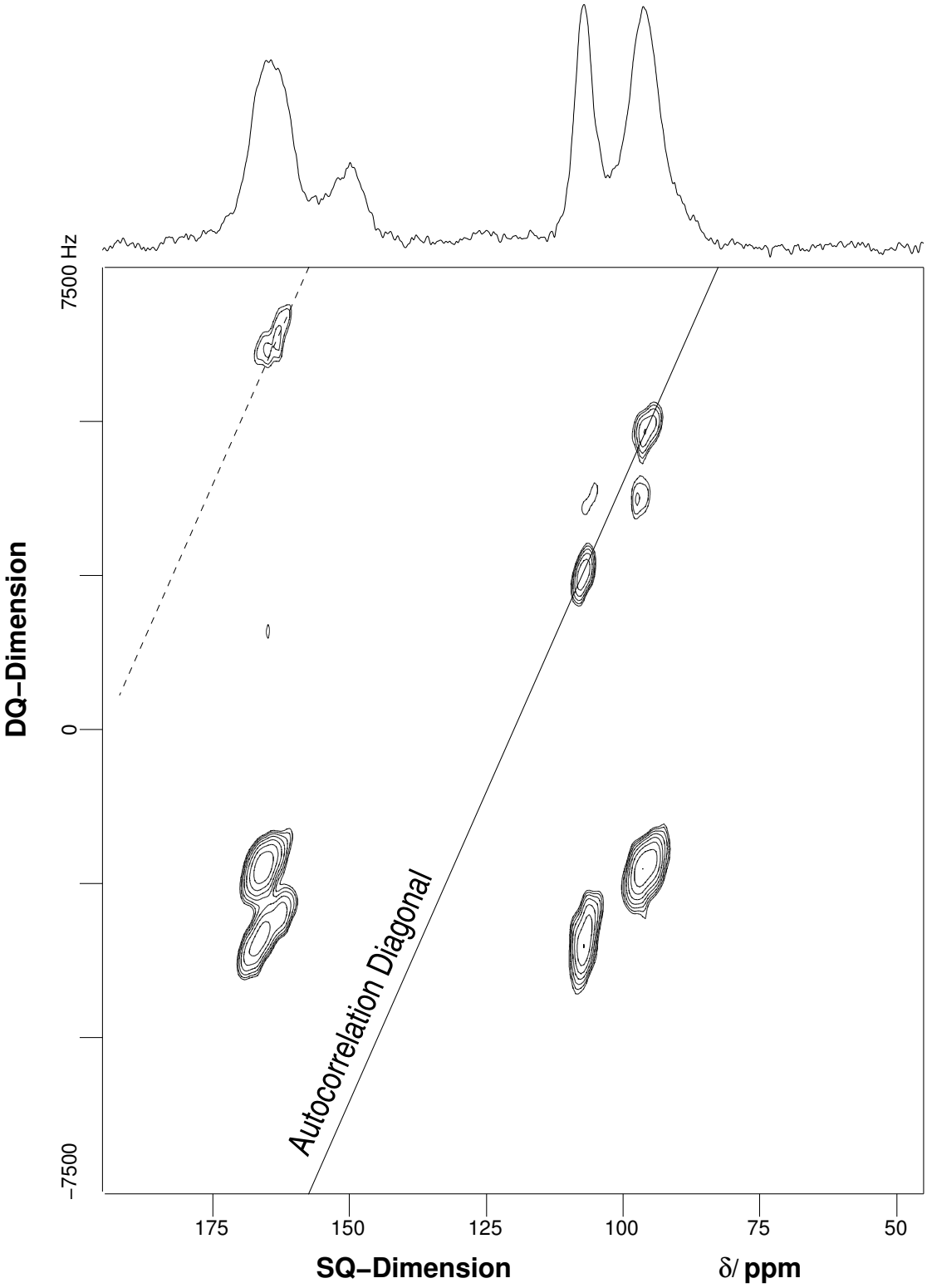

Figure 8: 2D double-quantum filtered correlation spectrum of poly(carbonsuboxide) (**sample II**) using the through-space dipolar coupling; the autocorrelation signal at 163 ppm is folded over the edge; the fold-over autocorrelation diagonal is indicated by a dashed line.

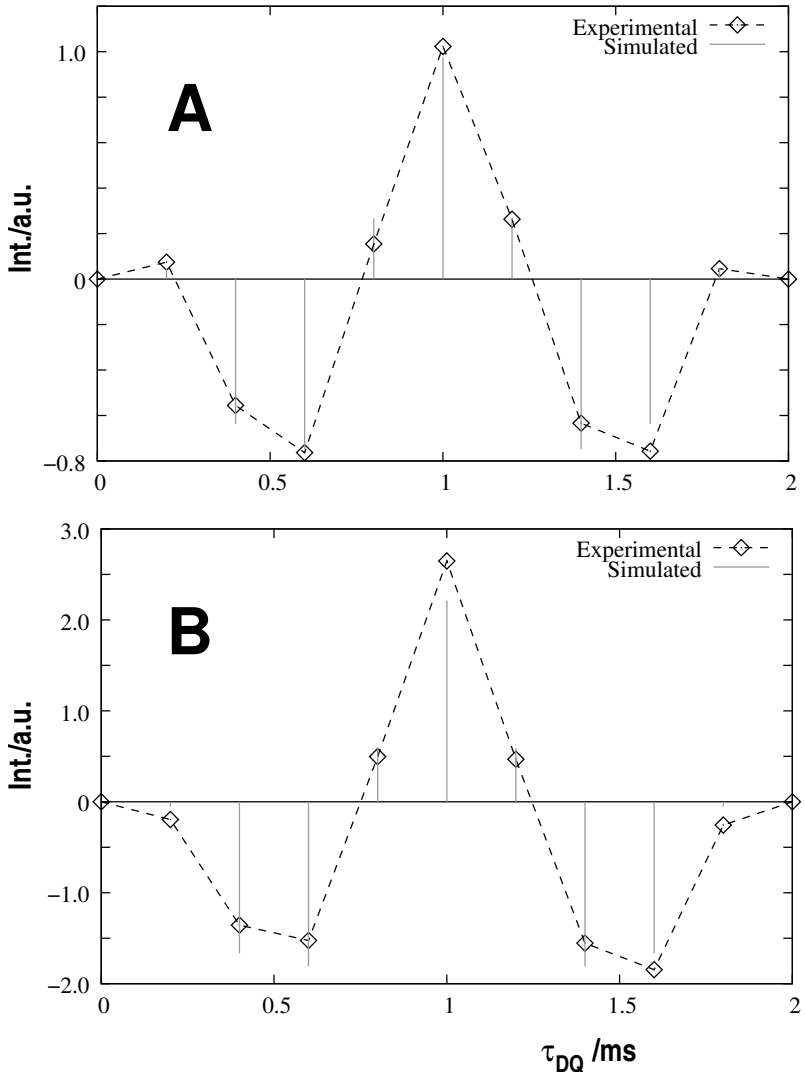

Figure 9: Double-quantum constant-time double-filtering build-up curves for the resonances at 107.5 ppm (lower curved labeled B) and 96 ppm (upper curve marked A) of poly(carbonsuboxide) (**sample II**), acquired at $\nu_r = 10$ kHz spinning-speed (pulse-sequence D, figure 2); if no double-filtering is applied no zero-crossings can be observed in double-quantum constant-time build-up curves.

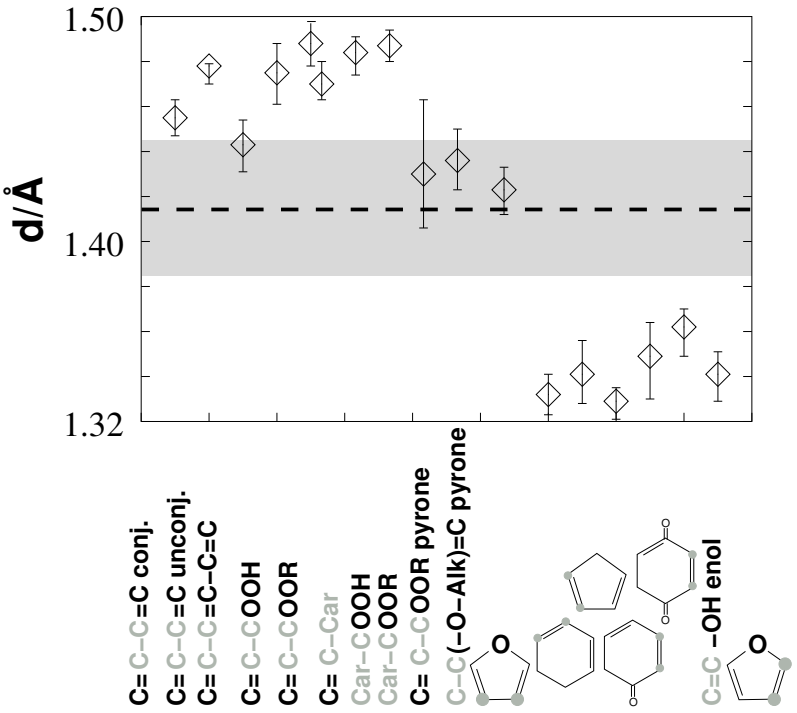

Figure 10: bond length distribution parameters for carbon-carbon bonds; data were graphically adapted from [45], additionally bond length parameters for α-pyrone and furan carbon fragments were determined with the help of the Cambridge Structural Database; plotted are mean d, lower and upper quartile (as error margins) for each bond type; the experimental value for the intermonomeric carbon-carbon distance (see figure 9) and its approximate error are indicated by the dashed line and the greyed area, respectively.

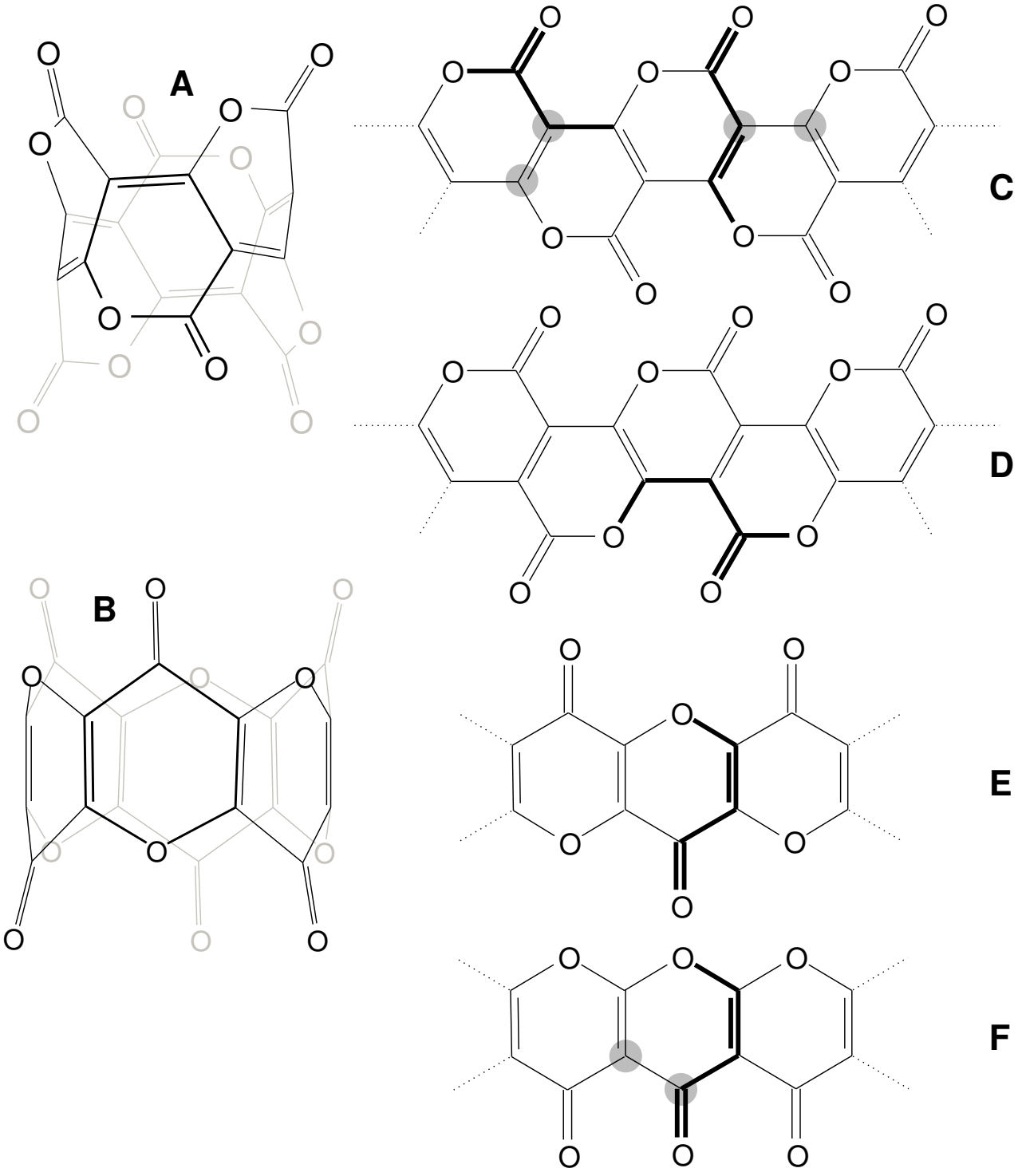

Figure 11: Model structures for poly(carbonsuboxide); marked in bold type are atoms belonging to the same monomer (structures C to F); the carbon atoms highlighted by grey circles refer to carbon atoms in an intermonomeric $C_{CCC} - C_{CCO}$ bond.